

4.3.4 Cone impinging a mesh boundary test results

Galerkin leaves trailing waves all over the domain, and when the cone has recently leaved the mesh, oscillations with a maximum height of 7.5% of the initial cone height remains. SUPG leaves minimum oscillations that exits the mesh rapidly, just behind the cone, with a maximum height of 7.1%. With the semi-Lagrangian method, the cone exits the mesh cleanly, with no oscillations, as can be seen in figure 8.

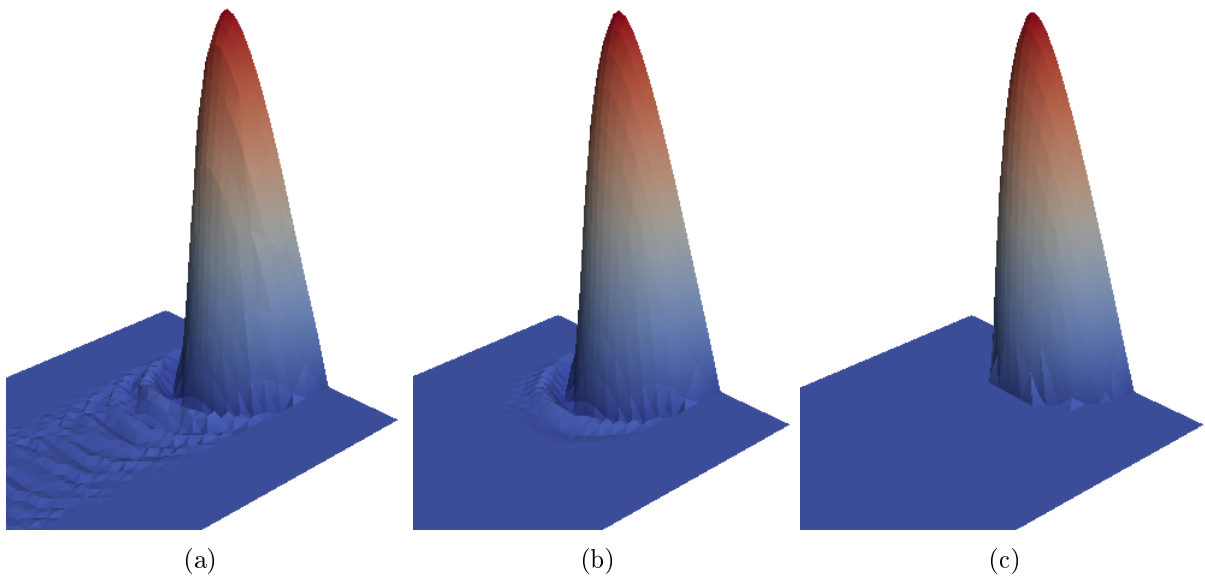


Figure 8 – Results after a full rotation: (a) Galerkin; (b) SUPG (c) semi-Lagrangian

In the previous test quadratic elements were used. It has been noticed in previous works with the semi-Lagrangian ((12), (25), (6)) that using lower order interpolation (even with fine meshes) gives very diffusive results. This can be seen in figure 9. This problems can be solved refining the mesh, as seen in figure 10. Here we have taken a mesh with the double of elements to compensate the lower order elements. But on the same mesh, with low order interpolation, the SUPG shows better results. We will return to this in section 4.4.4 .

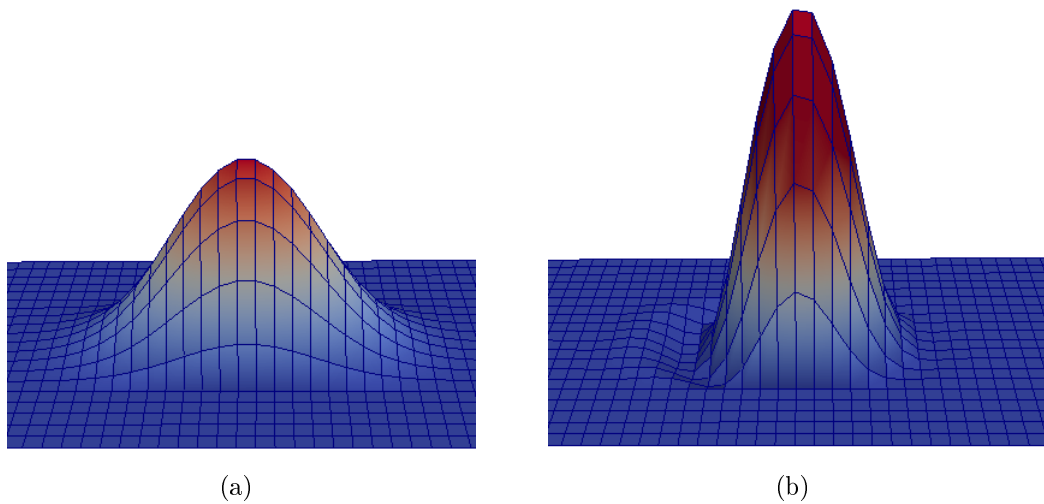


Figure 9 – Results on the cone impinging a mesh boundary (4 node quadrilaterals instead of 9). (a): semi-Lagrangian; (b) SUPG.

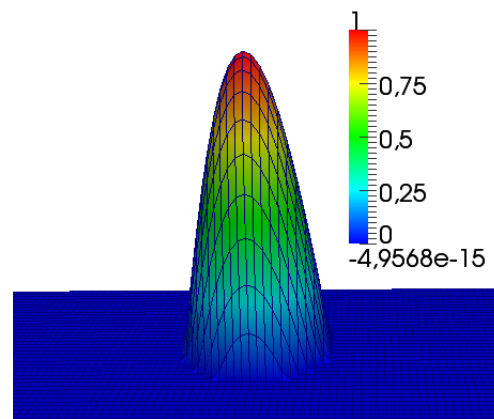


Figure 10 – semi-Lagrangian results with 4 node quadrilaterals and a finer mesh

4.4 Tests on the Navier-Stokes equations

4.4.1 The 2D lid-driven cavity test

In order to evaluate the characteristics of the semi-Lagrangian method and to test its feasibility in the context of high Reynolds numbers we analyze the lid-driven cavity problem, a well-known benchmark for N-S solvers. This flow is not only technologically important, it is of great scientific interest because it displays almost all fluid mechanical phenomena in the simplest of geometrical settings. Thus corner eddies, longitudinal vortices, nonuniqueness, transition and turbulence all occur naturally and can be studied in the same closed geometry. This facilitates the comparison of results

from experiment, analysis, and computation over the whole range of Reynolds numbers (26).

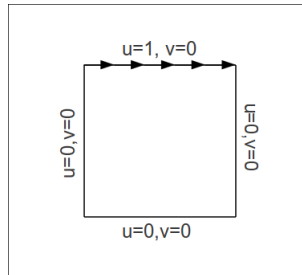


Figure 11 – Lid-driven cavity problem statement

The problem statement is shown in figure 11. It is a square cavity with no-slip boundary conditions, and velocity in the upper boundary is equal to 1 in the x direction. Pressure is pinned to zero in the lower left corner.

Erktuk et al. (27) solved the same problem using an streamfunction and vorticity formulation using finite differences in a very fine mesh of 601×601 elements. Hachem et al. (1) used an multiscale method for solving the same problem, over two meshes: a fine one of 180×180 elements, and an coarse one of 64×64 elements. Ghia et al. (28) applied a second-order accurate finite difference method using a fine grid of 257×257 . The work of Hachem has shown very good results compared with (27), even with a coarser mesh. We will refer mostly to the works of Hachem and Erkturk.

The meshes employed in our simulations are presented in figures 12 and 13. They are refined next to the boundary for better resolution of the boundary layer. This mesh is composed of triangular elements with quadratic interpolation for velocity, and linear interpolation for pressure (to satisfy the Babuska-Brezzi condition). Reynolds numbers of 1.000, 5.000 and 10.000 are established. For all of them, calculations are performed usings increasing CFLs of 1.1375, 1.52, 2.275 and 4.55, in order to compare the semi-Lagrangian versus the SUPG. Results are compared with those of (27) and (1).

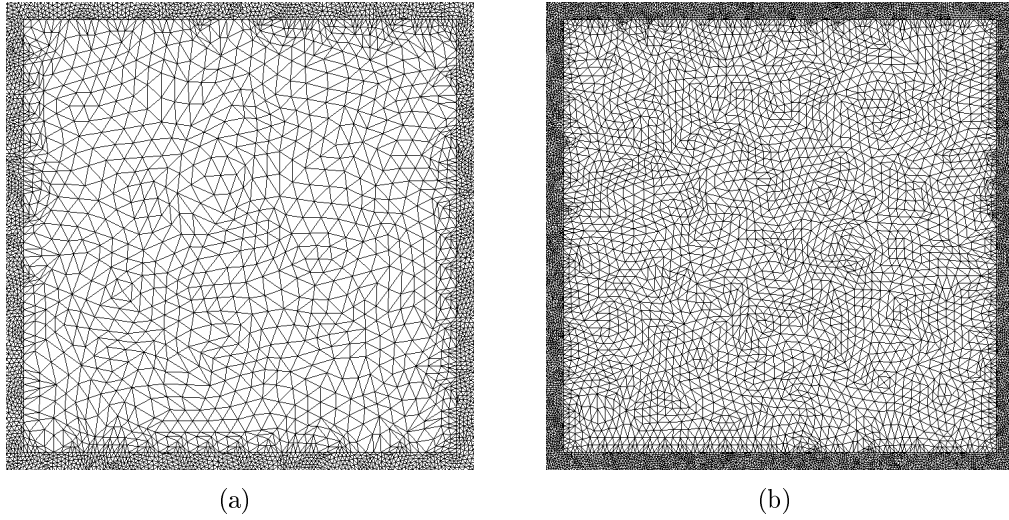


Figure 12 – Lid driven cavity 2D meshes: (a) 2.000 elements. (b) 5.000 elements.

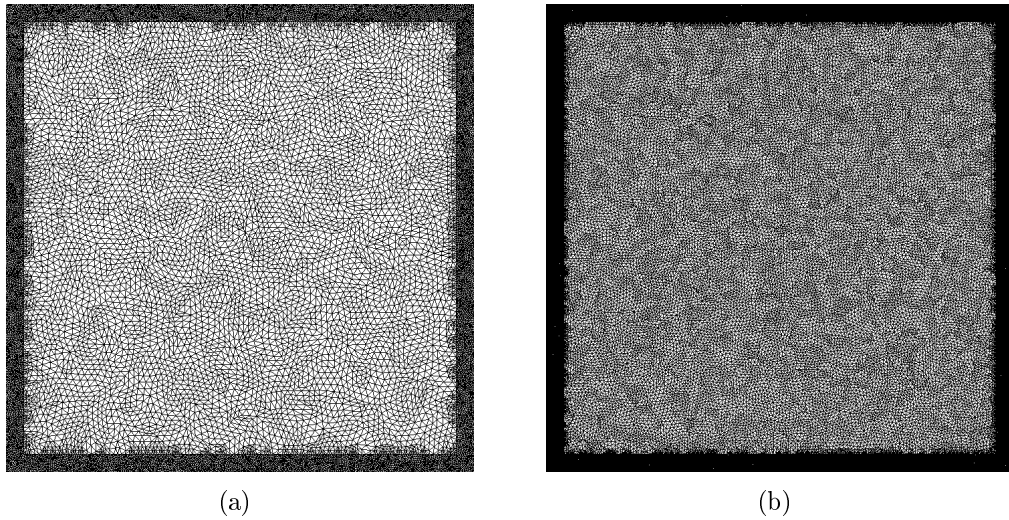


Figure 13 – Lid driven cavity 2D meshes: (a) 10.000 elements. (b) 40.000 elements.

We consider that steady state has been reached once the L2-norm of the normalized velocity difference between two timesteps is lower than $1.0e - 4$. Velocity profiles, position of vortex, streamline plots and graphics of error of the solutions (compared with a more accurate solution) are analysed, following the work of Hachem (1) and the verification and validation procedures seen in (29). The error of a certain simulation is computed as:

$$err(h) = \left(\sum_{x,y} (\mathbf{v}_{ref}^i - \mathbf{v}_k^i)^2 \right)^{\frac{1}{2}} \quad (4.1)$$

where h is making reference to a certain mesh and \mathbf{v}_{ref} is the velocity at the points of the reference mesh (the accurate solution). Comparison is made against the SUPG results computed with the finest mesh (40.000 elements).

4.4.2 2D lid-driven cavity test

Velocity profiles are shown in figures 15, 16 and 17. In those figures we expose extreme cases of resolution: our finer and our coarser mesh. Our results in the meshes with intermediate resolution (5.000 and 10.000 elements) have shown an intermediate adequacy (as expected) between the coarsest and the finest mesh results, and therefore are not exhibited. The very accurate solution from Erkturk (27) and our SUPG solution are plotted as well as the semi-Lagrangian method for several CFLs (equation 2.34) in order to show the influence of taking bigger time steps. As can be

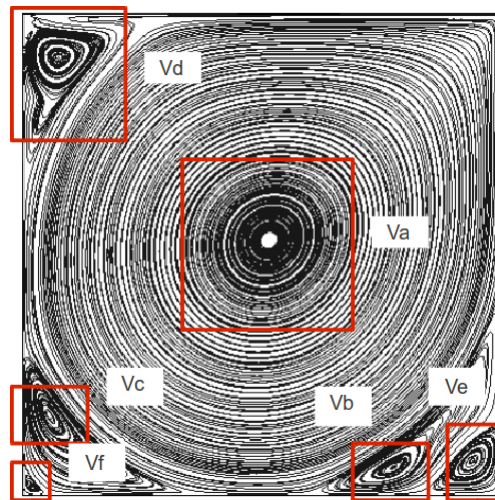


Figure 14 – Position of vortex until $Re=10.000$

seen, for low CFLs ($CFL \simeq 1.0$), semi-Lagrangian approximation is good, very close to the SUPG solution even for the highest Reynolds solution computed, however, the SUPG solution is slightly better comparing to (27). As the CFL grows, approximation becomes less accurate; this effect is more notorious when Reynolds number is higher; in this case $CFL \geq 3.0$ grants poor approximations. As the only parameter that is being changed in this test (for the same mesh and same Reynolds number) is Δt then we can see that the origin of the problem stated before is strongly associated to the linear trajectory used to approximate the material derivative in 3.1 .